A. INTERIM ANNUAL REPORT

Project ID: 2003OK17B

Title: Dual sensor for detecting xenobiotics and microorganisms

Project Type: Research

Focus Categories: Surface Water, Toxic Substances, Water Quality

Keywords: spectrophotometer, cytochrome P450, autofluorescence

Start Date: 03/01/2003

End Date: 02/28/2004

Federal Funds Requested: $25000.00

Matching Funds: $50000.00

Congressional District: 3rd

Principal Investigators: John, Gilbert; Rivera, Mario; Yen, Gary

Oklahoma Water Resources Research Institute (OWRRI)
July 2004

B. RESEARCH

INTRODUCTION:

Since September 11th, Homeland Security in the United States has become more important, as many aspects of security in this country are being examined and developed. One aspect is the security of drinking water. Deliberate contamination of drinking water make it imperative to have an efficient, sensitive, specific and rapid sensor that can detect both xenobiotics and microbial organisms that can cause harm to individuals. Billions of dollars are being made available from government and state agencies to develop systems that can continuously monitor drinking water. A multi-discipline group at Oklahoma State University is involved in developing a dual sensor that can be used in this capacity. Our proposal specifically addresses two critical areas that are important for further development of a dual sensor that can detect potentially harmful xenobiotics (toxicants) and pathogenic bacteria in water. The first area specifically addresses the issue of having stable proteins that can maintain their function under various environmental conditions. The cytochrome (CYP) P450 protein from the human liver is normally involved in

detoxifying and toxifying a broad range of xenobiotics, thereby CYP proteins can be used to directly link xenobiotics to human toxicity. A number of isoforms are present in the liver, but some of these proteins are not stable (CYP3A4), compared to stable proteins (CYP1A2). Therefore, the first area we addressed was to develop a method of improving stability of CYP 3A4 using molecular modeling techniques thereby increasing ion-pair interactions in the protein. The second area addressed was to examine the autofluorescence signatures (spectrofluorimetry) from bacteria, which may provide a means of identifying different types of bacterial pathogens. Available methods that can be used to improve the stability of cytochrome P450 without compromising function as well as having unique spectra that can be used to specifically identify potentially harmful pathogens is critical for future development of a dual sensor.

The research report addresses two areas, 1.) development of a computer graphics method for improving protein stability, which will enable the proteins to effectively detect potentially harmful xenobiotics and 2.) to determine if autofluorescence signatures from whole bacteria can be used to detect pathogenic bacteria in water.

METHODS AND RESULTS

Area 1.) To improve the stability of cytochrome P450 proteins for use in detecting xenobiotics, a computer graphics-modeling program was necessary in order to determine the important residues involved in protein stability. Three graphics programs were identified to have functions that were relevant and applicable to the project. They included PyMOL (Delano Scientific, http://www.delanoscientific.com), DeepView(Swiss Model), and WHAT IF Web Interface). Computer modeling coordinates for CYP 1A2 and 3A4 were used to generate the protein models and were obtained from Dr. Lewis (United Kingdom). The mutant protein model was tested for distances (residue positions based on 3-D images) using PyMOL prior to submitting the model for residue alteration by the WHAT IF server. Since the computer model of CYP 1A2 and 3A4 were similar, the mutational prediction for 3A4 was possible based on the analysis of the hydrogen bonds networks and ion pair networks of the CYP 1A2. Mutations were predicted based the method of Chinea.G & Vriend.G, for position-specific rotamers (14). The WHAT IF web interface calculates distances in angstroms (15).

The computational analysis allowed the selection of five candidates for site-directed mutagenesis of the CYP 3A4. The candidates were selected based on the number of additional ion pairs, hydrogen bonds, and additional residue interactions that were created based on the model and data received from the WHAT IF web interface.

Different stabilities exist within the family of cytochromes (CYP). Therefore, we hypothesize that some of the stability is due to ion pairs and/or ion networks (1-7). WHAT IF (http://swift.cmbi.kun.nl/WIWWWI/), a web server, was used to locate the number of optimal hydrogen bonds networks and salt bridge locations within the proteins according to the protein data bank files. Using the computer graphics programs, it was shown that the wildtype CYP 1A2 (more stable) had more ion pair networks than CYP 3A4 (less stable). To improve CYP 3A4 stability, residues distant from the substrate-binding region were selected for site-directed mutagenesis. Figure 1 shows the five selection residues selected for mutation, based on the superimposition generated by PyMOL. Figure 2 shows the GLU66=>ASP66 change, which increases the salts bridges (ion pairs) from 2 to 3, as well as providing a supporting hydrogen bond network (Table

1 and 2). Figure 3 shows the VAL124=>LYS124 change, which increases the salt bridges from 0 to 4 and maintains supporting hydrogen bond networks (Table 3 and 4). Figure 4 shows the GLY146=>ARG146 change, which increases the salt bridges from 0 11 and maintains supporting hydrogen bond networks (Table 5 and 6). Figure 5 shows the TYR376=>HIS376 change, which increases the salt bridges from 0 to 5 and maintains supporting hydrogen bond networks (Table 7 and 8). Figure 6 shows the ASN431=>ASP431 change, which increases the salt bridges from 0 to 3 and maintains supporting hydrogen bond networks (Table 9 and 10). Incorporation of all or selected mutations will be tested.

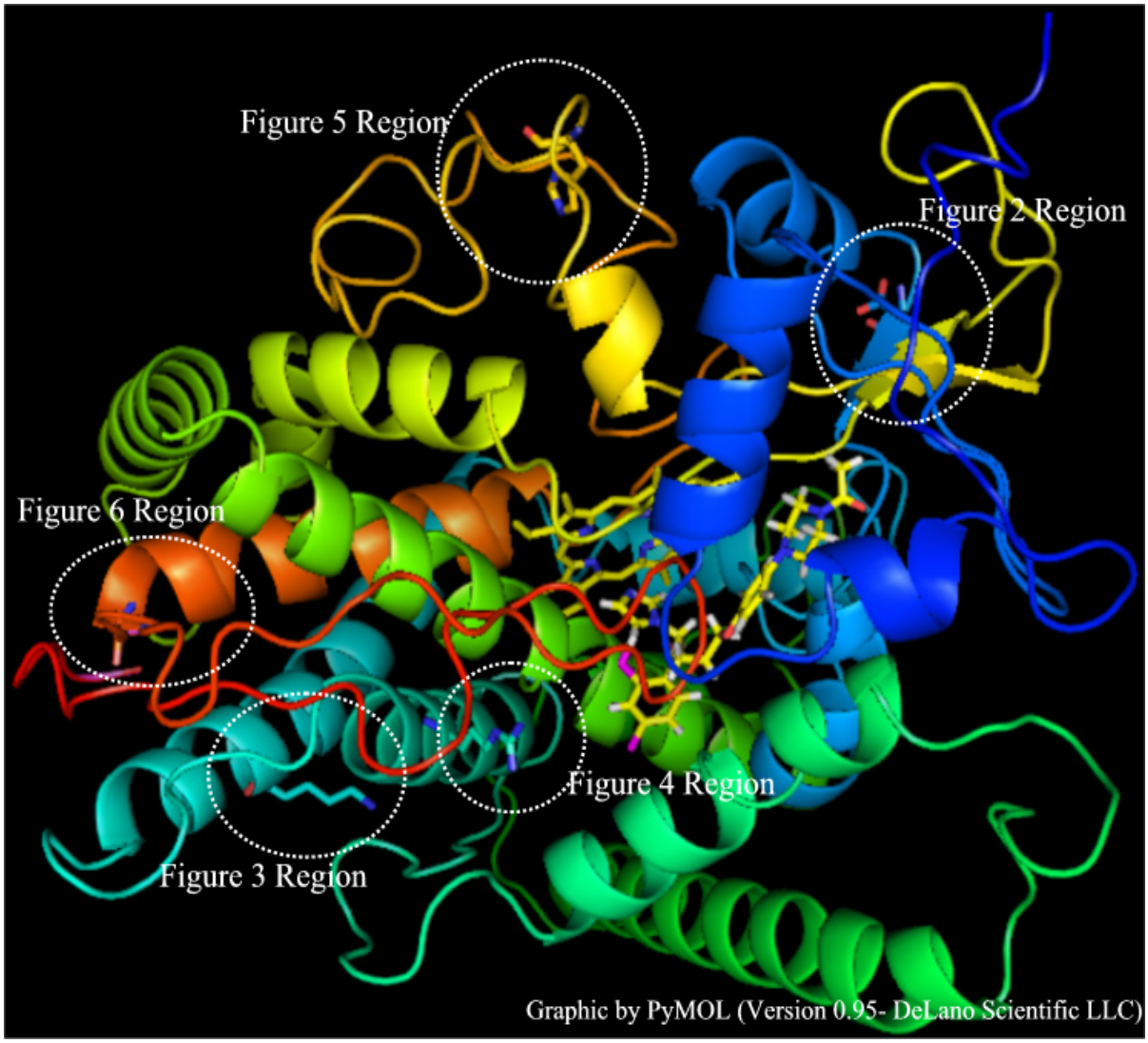

Figure 1: Superimposition of wild-type (wt) CYP3A4 and Mutant (m3a4) illustrating entire enzyme structure*.

a. Each ellipse corresponds to a mutant containing region.
b. Mutant residues are seen above as sticks.

* Graphic by PyMOL DeLano Scientific LLC & Edited with Microsoft PhotoDraw for all figures.

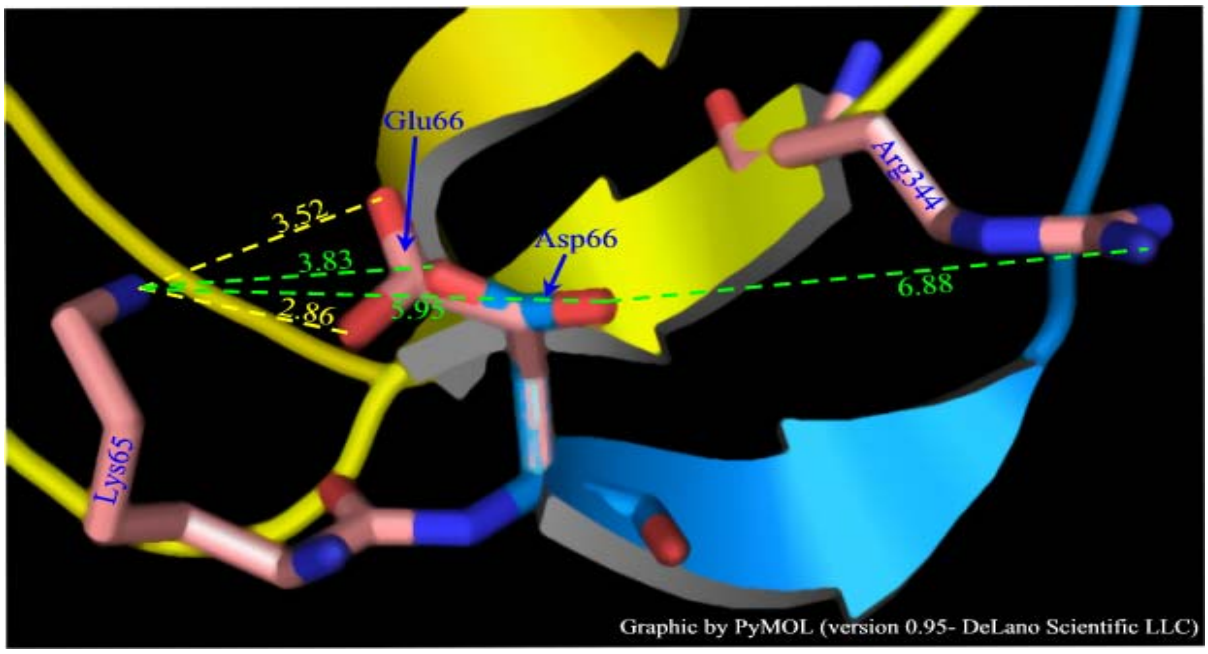

Fig. 2: Superimposition of wt- Glu66** and Mutant- Asp66 (m66)

a. m66 shown in blue sticks entangled with Glu66 pink
b. Ionic interaction- wt in yellow and m66 in green
c. Ionic interaction distance is in Å.
d. Residues Lys60, Thr61, Val62, Leu63, & Val64 were removed for clarity.

Table 1: WHAT IF- Salt Bridge Data (SBD), mutant data in boldface

Donor Residue	Donor Molecule	Acceptor Residue	Acceptor Molecule	Distance (Å)
66 ASP (66)	**OD1**	**65 LYS (65)**	**NZ**	**5.95**
66 ASP (66)	**OD2**	**65 LYS (65)**	**NZ**	**3.83**
66 ASP (66)	**OD1**	**344 ARG (344)**	**NH2**	**6.88**
66 GLU (66)	OE1	65 LYS (65)	NZ	3.52
66 GLU (66)	OE2	65 LYS (65)	NZ	2.86

Table 2: WHAT IF- Optimal Hydrogen Bond Network Data (OHBD), mutant data in boldface

Donor Residue	Donor Molecule	Acceptor Residue	Acceptor Molecule	Hydrogen Bond Value (0.0-1.0)[a]	Distance (Å)
65 LYS (65)	**NZ**	**-> 66 ASP (66)**	**OD2**	**Val= 0.437**	**DA= 3.83**
65 LYS (65)	N	-> 66 GLU (66)	OE2	Val= 0.390	DA= 2.85
65 LYS (65)	NZ	-> 66 GLU (66)	OE2	Val= 0.653	DA= 2.86

a. estimated importance of hydrogen bonds relative to each other. Perfect hydrogen bond = 1.0.

** Residue numbers based on coordinate file data for sequence residue numbers add thirty-two (32) for all data.

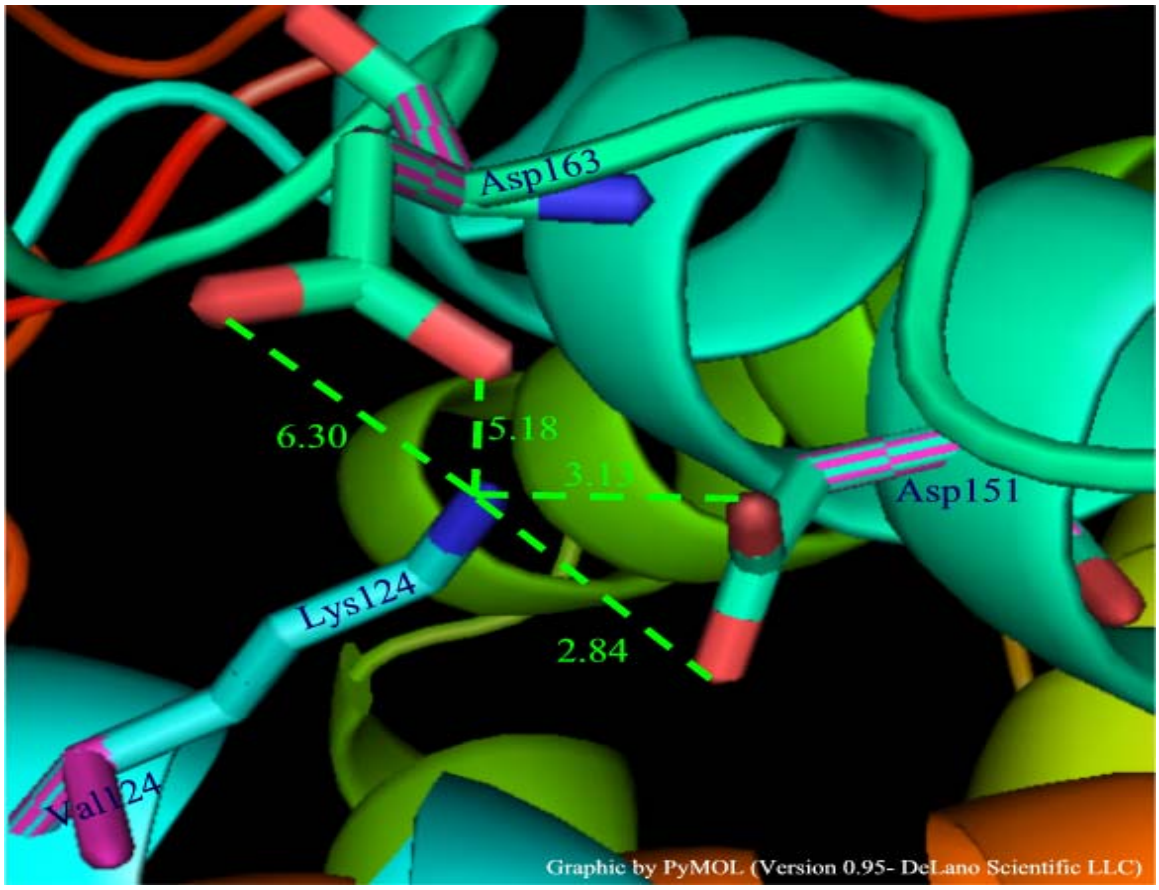

Figure 3: Superimposition of wt-Val124 and Mutant- Lys124 (m124)

a. m124 shown through Val124 striped, other stripes show superimposed residues.
b. Ionic interaction- wt-null and m124 in green
c. Ionic Interaction distance (green) in Å.

Table 3: WHAT IF- SBD

Donor Residue	Donor Molecule	Acceptor Residue	Acceptor Molecule	Distance (Å)
151 ASP (151)	**OD1**	**124 LYS (124)**	**NZ**	**3.13**
151 ASP (151)	**OD2**	**124 LYS (124)**	**NZ**	**2.84**
163 ASP (163)	**OD1**	**124 LYS (124)**	**NZ**	**5.18**
163 ASP (163)	**OD2**	**124 LYS (124)**	**NZ**	**6.30**

Table 4: WHAT IF - OHBN

Donor Residue	Donor Molecule	Acceptor Residue	Acceptor Molecule	Hydrogen Bond Value (0.0-1.0)[a]	Distance (Å)
124 LYS (124)	**N ->**	**120 GLN (120)**	**O**	**Val= 0.706**	**DA= 2.99**
128 ASN (128)	**N ->**	**124 LYS (124)**	**O**	**Val= 0.607**	**DA= 2.82**
124 VAL (124)	N ->	120 GLN (120)	O	Val= 0.706	DA= 2.99
128 ASN (128)	N ->	124 VAL (124)	O	Val= 0.607	DA= 2.82

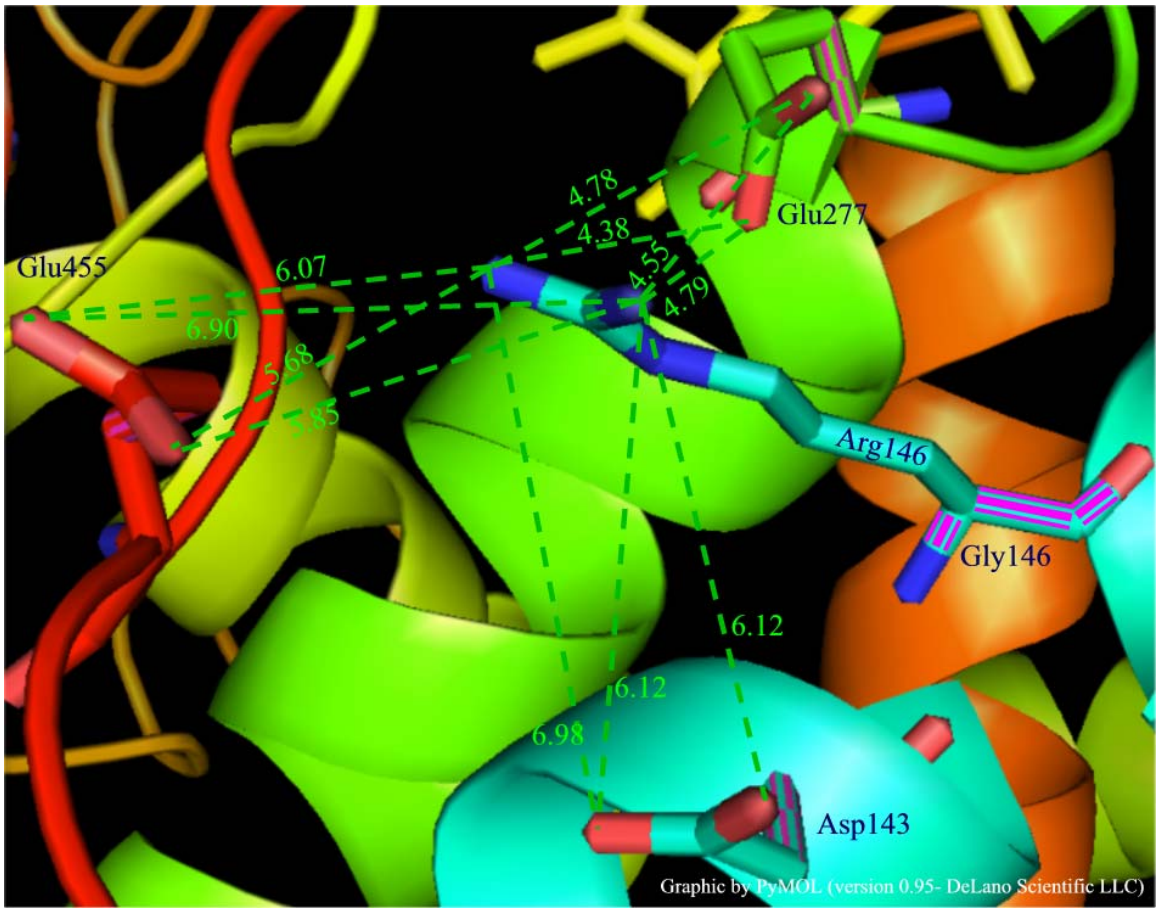

Figure 4: Superimposition of wt-Gly146 and Mutant- Arg146 (m146)

a. m146 shown through Gly146 striped, other stripes show superimposed residues.
b. Ionic interaction- wt-null and m146 in green
c. Ionic interaction distance (green) in Å.
d. Cartoon of main chain for wt and m146 has been removed at residue 146 for clarity.

Table 5: WHAT IF- SBD

Donor Residue	Donor Molecule	Acceptor Residue	Acceptor Molecule	Distance (Å)
143 ASP (143)	**OD1**	**146 ARG (146)**	**NH1**	**6.12**
143 ASP (143)	**OD1**	**146 ARG (146)**	**NH2**	**6.98**
143 ASP (143)	**OD2**	**146 ARG (146)**	**NH1**	**6.12**
277 GLU (277)	**OE1**	**146 ARG (146)**	**NH1**	**4.55**
277 GLU (277)	**OE1**	**146 ARG (146)**	**NH2**	**4.78**
277 GLU (277)	**OE2**	**146 ARG (146)**	**NH1**	**4.79**
277 GLU (277)	**OE2**	**146 ARG (146)**	**NH2**	**4.38**
455 GLU (455)	**OE1**	**146 ARG (146)**	**NH1**	**6.90**
455 GLU (455)	**OE1**	**146 ARG (146)**	**NH2**	**6.07**
455 GLU (455)	**OE2**	**146 ARG (146)**	**NH1**	**5.85**
455 GLU (455)	**OE2**	**146 ARG (146)**	**NH2**	**5.68**

Table 6: WHAT IF- OHBN

Donor Residue	Donor Molecule	Acceptor Residue	Acceptor Molecule	Hydrogen Bond Value (0.0-1.0)[a]	Distance (Å)
146 ARG (146)	**N ->**	**142 LYS (142)**	**O**	**Val= 0.629**	**DA= 3.19**
146 ARG (146)	**N ->**	**143 ASP (143)**	**O**	**Val= 0.090**	**DA= 3.04**
150 MET (150)	**N ->**	**146 ARG (146)**	**O**	**Val= 0.743**	**DA= 3.06**
146 GLY (146)	N ->	142 LYS (142)	O	Val= 0.629	DA= 3.19
146 GLY (146)	N ->	143 ASP (143)	O	Val= 0.090	DA= 3.04
150 MET (150)	N ->	146 GLY (146)	O	Val= 0.743	DA= 3.06

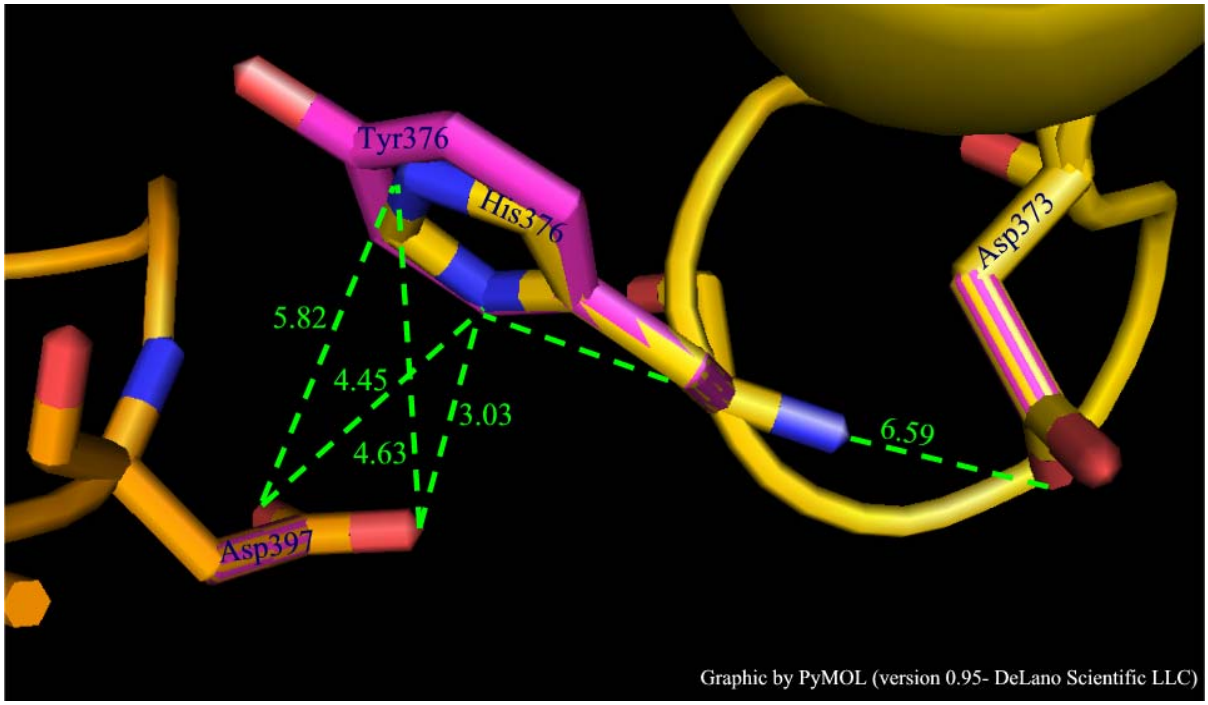

Figure 5: Superimposition of wt- Tyr376 and Mutant- His 376 (m376)

a. m376 shown entangled inside Tyr376 purple, other stripes show superimposed residues.
b. Ionic interaction- wt-null and m376 in green
c. Ionic interaction distance (green) in Å.
d. Residues Ile 365 & 400 removed for clarity.

Table 7: WHAT IF- SBD

Donor Residue	Donor Molecule	Acceptor Residue	Acceptor Molecule	Distance (Å)
373 ASP (373)	**OD1**	**376 HIS (376)**	**ND1**	**6.59**
397 ASP (397)	**OD1**	**376 HIS (376)**	**ND1**	**4.45**
397 ASP (397)	**OD1**	**376 HIS (376)**	**NE2**	**5.82**
397 ASP (397)	**OD2**	**376 HIS (376)**	**ND1**	**3.03**
397 ASP (397)	**OD2**	**376 HIS (376)**	**NE2**	**4.63**

Table 8: WHAT IF- OHBN

Donor Residue	Donor Molecule	Acceptor Residue	Acceptor Molecule	Hydrogen Bond Value (0.0-1.0)[a]	Distance (Å)
376 HIS (376)	**N ->**	**373 ASP (373)**	**OD1**	**Val= 0.666**	**DA= 3.19**
376 HIS (376)	**ND1 ->**	**397 ASP (397)**	**OD2**	**Val= 0.233**	**DA= 3.03**
376 TYR (376)	N ->	373 ASP (373)	OD1	Val= 0.666	DA= 3.19
376 TYR (376)	OH ->	397 ASP (397)	O	Val= 0.354	DA= 3.42

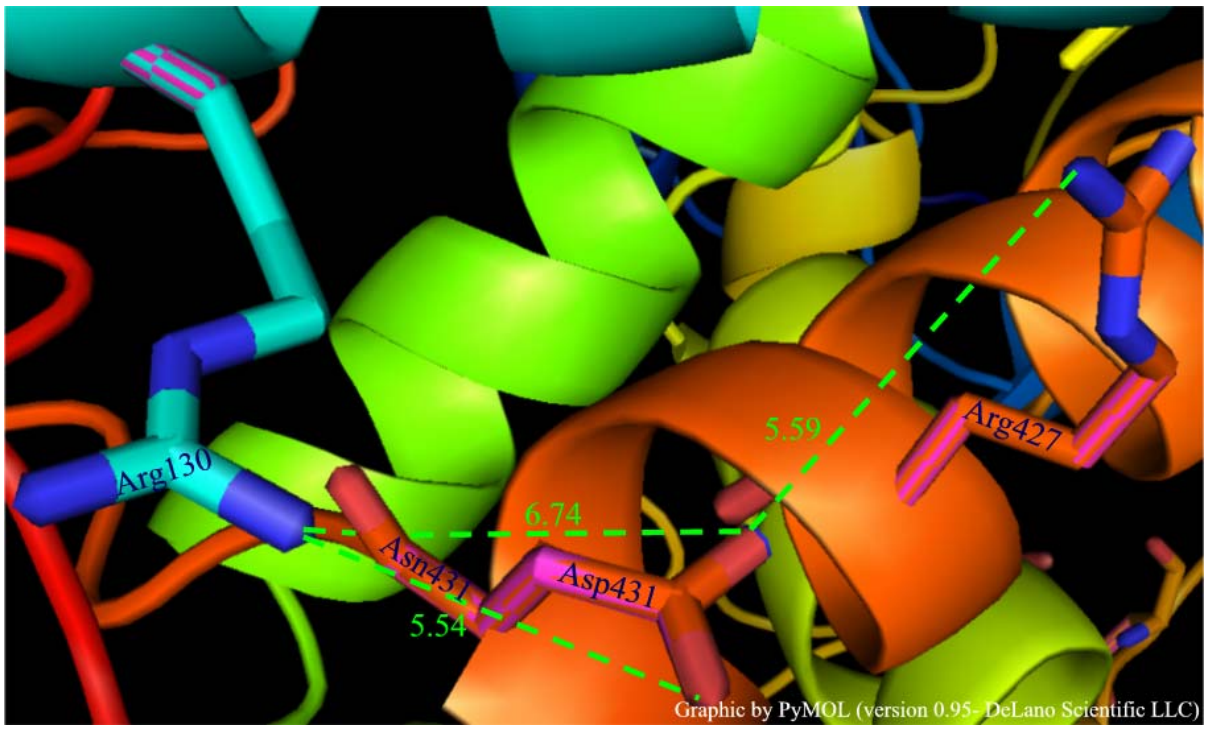

Figure 6: Superimposition of wt- Asn431 and Mutant- Asp431 (m431)

a. m431 red shown entangled inside Asn431 purple, other stripes show superimposed residues.
b. Ionic interaction- wt-null and m431 in green
c. Ionic interaction distance (green) in Å.
d. Residues Thr468 &Val469 removed for clarity.

Table 9: WHAT IF- SBD

Donor Residue	Donor Molecule	Acceptor Residue	Acceptor Molecule	Distance (Å)
431 ASP (431)	**OD1**	**130 ARG (130)**	**NH1**	**6.74**
431 ASP (431)	**OD2**	**130 ARG (130)**	**NH1**	**5.54**
431 ASP (431)	**OD1**	**427 ARG (427)**	**NH2**	**5.59**

Table 10: WHAT IF- OHBN

Donor Residue	Donor Molecule	Acceptor Residue	Acceptor Molecule	Hydrogen Bond Value (0.0-1.0)[a]	Distance (Å)
430 GLN (430)	**NE2 ->**	**431 ASP (431)**	**OD1**	**Val= 0.602**	**DA= 2.99**
431 ASP (431)	**N ->**	**427 ARG (427)**	**O**	**Val= 0.538**	**DA= 2.80**
465 LYS (465)	**N ->**	**431 ASP (431)**	**O**	**Val= 0.520**	**DA= 3.14**
431 ASN (431)	N ->	427 ARG (427)	O	Val= 0.538	DA= 2.80
431 ASN (431)	ND2 ->	430 GLN (430)	OE1	Val= 0.610	DA= 3.02
431 ASN (431)	ND2 ->	427 ARG (427)	O	Val= 0.416	DA= 2.85
465 LYS (465)	N ->	431 ASN (431)	O	Val= 0.520	DA= 3.14

Area 2: The stability of the autofluorescence signature for *E. coli* was analyzed based on exposure to Carvacrol, a phenolic compound present in oregano and thyme plant essential oils. *E coli* strain C600 (ATCC 47024) (a gift of Moses Vijayakumar, Oklahoma State University), and E. coli O157:H7 (two different strains) were frozen at -80°C in a Trypticase Soy Broth (TSB) containing a final concentration of 15% glycerol. For use in experiments, a 100 µl sample of thawed stock was inoculated into 100 ml TSB and incubated at 37 °C overnight in a shaker bath at 120 rpm.

A monochromatic-based spectrofluorimeter (Photon Technology, Princeton, NJ, USA) was used for fluorescence. This instrument uses a xenon arc lamp to illuminate a one-half meter monochromator. The output of the monochromator is focused on a sample chamber wherein a sample cuvette is placed. Emission from the sample cuvette was collected at an angle of 90 degrees to the excitation after passing through an emission monochromator. Collection of the data was performed using photon-counting and a Hammamatsu R920 photomultiplier tube. Photon counts were stored on magnetic media and later analyzed and plotted using S-Plus (Insightful, Seattle, WA, USA) and Prism. A digital filter was applied to the raw data to remove photon scatter less than 25 nm of the absolute value of the excitation wavelength less the emission wavelength. An additional digital filter was applied to the data to remove the emissions from doubling of the primary excitation wavelength.

For culture preparation, a 3 ml of the overnight culture was mixed and removed from the middle of the flask and centrifuged at 2000 X g for 5 min. The resulting supernatant was removed and the pellet was resuspended in 150 mM saline. After a second centrifugation at 2000 X g, the pellet was resuspended in 3.0 ml of either control (150 mM NaCl, 2% EtOH) or treatment (0.01, 0.1, 1.0 mM carvacrol, 15.0 mM NaCl, 2% EtOH) in a polystyrene fluorimeter cuvette. Both control and treatment samples were maintained at room temperature. Optical density (absorbance at 660 nm) measurements (Ocean Optics S2000, Ocean City, MD, USA) were performed on each treatment before and after measuring autofluorescence to insure equivalent numbers of bacteria in control and treatment samples. After 15 min of incubation at room temperature in either control or carvacrol treatment, the cuvette containing the bacterial sample was placed in the sample chamber of a spectrofluorimeter (Photon Technology, Princeton, NJ, USA) and fluorescence was measured using excitation wavelengths of 300-700 nm and 400-700 nm emission. Fluorescence data was acquired by a computer, stored on magnetic media, and processed as three-dimensional plots using S-Plus (Insightful, Seattle, USA). All fluorescence scans were referenced to a factory fluorescent-calibration standard (Photon Technology Inc, Princeton, NJ, USA).

Figure 7 represents autofluorescence data from *E. coli* that was treated without carvacrol (control) or various concentrations of carvacrol. One axis of Figure 7 represents the excitation wavelength, which varied from 300 nm to 700 run, and the second axis represents the emission wavelength, which varied from 400 nm to 700 nm. The vertical axis of Figure 7 represents the fluorescence from the bacterial sample and is in volts, representing the number of photons emitted. Figure 7 is divided into four panels representing the control autofluorescence and the autofluorescence of *E. coli* exposed to increasing concentrations of carvacrol. Figure 7A, the control autofluorescence panel, shows complex peaks of autofluorescence uniquely characteristic of the C600 strain of *E. coli* and a characteristic trough near 550 nm emission for all excitation wavelengths. Figures 7B, 7C, and 7D autofluorescence data from E. coli treated with 0.01 mM carvacrol, shows little change in the overall signature based on the

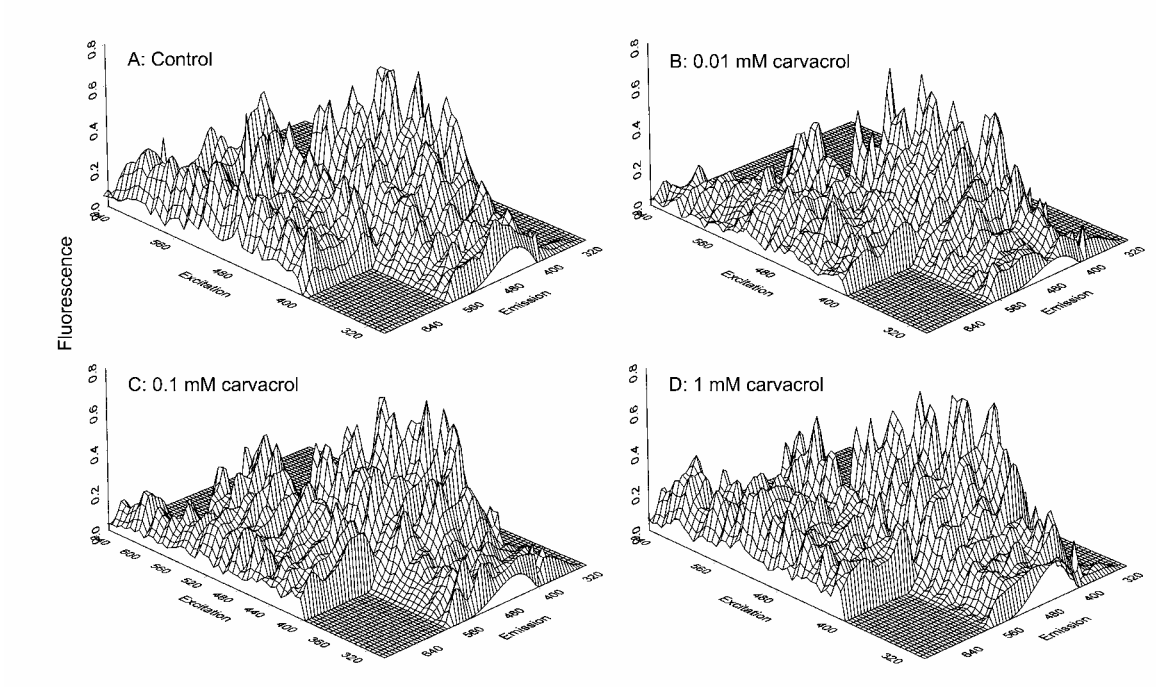

Figure 7. Three-dimensional representation of autofluorescence of E. coli exposed to the control (Fig. 7A) and 0.01 (Fig. 7B), 0.1 (Fig. 7C), and 1.0 mM (Fig. 7D) carvacrol. Excitation (axis leading away from observer and marked Excitation) ranged from 300 to 700 nm while emission (axis appearing flat) ranged from 400 to 700 nm.

We also presented the results as subtractions between control and treatments (difference spectra) in the panels of Figure 8. Figure 8A shows a control autofluorescence. Fig. 8B is the algebraic difference between the control autofluorescence spectrum and the 0.01 mM carvacrol spectrum (see Figure. 7B).

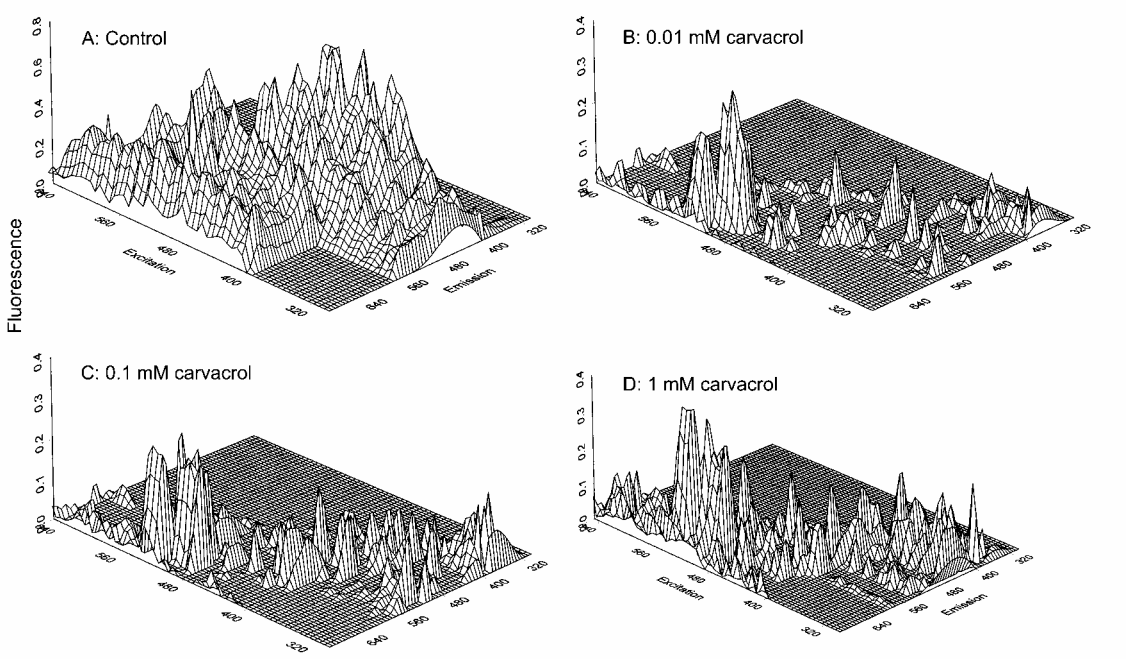

Figure 8. Three-dimensional representation of the autofluorescence of E. coli with control subtracted from each of the treatments (difference spectra): (Fig. 8A), control; (Figure 8B), 0.01 mM carvacrol less control; (Figure 8C), 0.1 mM carvacrol less control; and (Figure 8D), 1.0 mM carvacrol less control.

Although some changes did occur based on exposure to carvacol, overall there are peaks that remain stable, which is represented by flat or no peak formations in figures B, C, and D. Therefore, a stable autofluorescence signature for *E. coli* exist.

Further analysis of spectra data involved using the neural network system (13). Neural networks, an emerging machine learning approach, can perform highly complex mappings on noisy and nonlinear data, thereby inferring subtle relationships between sets of input and output parameters. They can in addition generalize from a limited quantity of training data to overall trends in functional relationships. Although several network architectures and training algorithms are available, the back-propagation type remains the most popular in bioinformatics applications (3). Feed-forward neural networks trained by back-propagation algorithm consist of several layers of simple processing elements called neurons, interconnections, and weights that are assigned to the interconnections. These rudimentary processors are interconnected in such a way that information relevant to the input-output mapping is stored implicitly in the weights. Each neuron contains the weighted sum of its inputs filtered by a sigmoid transfer function, endowing neural networks with the ability to generalize with an added degree of freedom not available in any statistical regression techniques. The input layer of neurons receives the external information such as the difference spectrum. The output layer transmits information to the outside world and this corresponds to the specific xenobiotics binded. Back-Propagation networks also incorporate one or more hidden layers of neurons which do not interact with the outside world, but assist in performing classification and nonlinear feature extraction tasks on information provided by the input and output layers. Neural network can be easily implemented in software, hardware or firmware, as appropriate.

The ability of real-time processing, noise rejection and continuous learning when more data become available make it a perfect tool for data analysis proposed herein. A nonpathogenic and two different strains of a pathogenic *E. coli* culture were analyzed using scanned data information. The different scans were analyzed and compared based on the number of data points having the same outputs (with a 5% threshold), which demonstrated a metric for comparison similar to regression analysis or sum square error analysis. Approximately 30% commonality exist between nonpathogenic and pathogenic *E. coli* (Table I). Approximately 60% commonality exist between the two strains of pathogenic *E. coli* (Table I). Based on the results, a distinction between nonpathogenic and pathogenic bacteria can be made. In addition, there is sufficient difference between the different stains of pathogens.

Table I

Percentage of commonality between scan 1, scan 2 & scan 3 of DISK 765

Scan 1 and scan 2	Scan 1 and scan 3	Scan 2 and scan 3	Scan 1,scan 2 & scan 3
30.22 %	30.15 %	60.62 %	30.15 %

Conclusion:

1.) Computer graphics modeling programs were used to determine the most ideal residues for mutation in order to increase stability of the CYP 3A4 protein. Future CYP proteins can be modified using the developed method.
2.) An emission/excitation spectrometer was build to generate 3-D plots from different species of bacteria. Nonpathogeneic and pathogenic strains of bacteria were tested. The results support the potential of autofluourescence signatures serving as method of identifying and distinguishing between different types of bacteria
3.) The preliminary data generated has enabled the submission of a larger grant to the National Science Foundation (Sensors and Sensor Networks), Program Solicitation NSF 03-512. Pending.

Reference:

1. Domanski, T.L., He, Y., Harlow, G.R. & Halpert J.R. (2000) Dual Role of Human Cytochrome P450 3A4 Residue Phe-304 in Substrate Specificity and Cooperativity. *JPET, 293*,2: 585-591.
2. Fowler, S.M., Taylor, J.M., Friedberg, T., Wolf, C.R. & Riley, R.J. (2002) CYP3A4 Active Site Volume Modification by Mutagenesis of Leucine 211. *Drug Metabolism and Disposition 30*,4: 452-456.
3. He, Y.A, He, Y.Q., Szklarz, G.D. & Halpert, J.R. (1997) Identification of Three Key Residues in Substrate Recognition Site 5 of Human Cytochrome

P450 3A4 by Cassette and Site-Directed Muagenesis. *Biochem. 36*, 29: 8831-8839.

4. He, Y.A., Roussel, F. & Halpert, J.R. (2003) Analysis of homotropic and heterotropic cooperativity of diazepam oxidation by CYP3A4 using site-directed mutagenesis and kinetic modeling. *Arch. Biochem. Biophys 409*: 92-101.
5. Khan, K.K., He, Y.Q., Domanski, T.L. & Halpert, J.R. (2002) Midzolam Oxidation by Cytochrome P450 3A4 and Active-Site Mutants: an Evaluation of Multiple Binding Sites and of the Metabolic Pathway That Leads to Enzyme Inactivation. *Mol. Pharmacol. 61*: 495-506.
6. Torimoto, N., Ishii, I., Hata, M., Nakamura, H., Imada, H., Ariyoshi, N., Ohmori, S., Igarashi, T. & Kitada, M. (2003) Direct Interaction between Substrates and Endogenous Steroids in the Active Site May Change the Activity of Cytochrome P450 3A4. *Biochem. 42*,51: 15068-15077.
7. Stevens, J.C., Domanski T.L., Harlow, G.R., White, R.B., Orton, E. & Halpert, J.R. (1999) Use of the Steroid Derivative RPR 106541 in Combination with Site-Directed Mutagenesis for Enhanced Cytochrome P-450 3A4 Struture/Function Analysis. *JPET, 290*, 2: 594-602.
8. Albrecht-Buehler, G. (1997) Autofluorescence of live purple bacteria in the near infrared. *Experimental Cell Research* **236,** 43-50.
9. Bergonzelli, G. E., Donnicola, D., Porta, N. and Corthesy-Theulaz, I. E. (2003) Essential oils as components of a diet-based approach to management of Helicobacter infection. *Antimicrobial Agents and Chemotherapy* **47,** 3240-3246.
10. Friedman, M., Henika, P. R. and Mandrell, R. E. (2002) Bactericidal activities of plant essential oils and some of their isolated constitutents against *Campylbacter jejuni*, *Escherichia coli*, *Listeria monocytogenes*, and *Salmonella enterica*. *Journal of Food Protection* **65,** 1545-1560.
11. Plettenberg, H. K. and Hoffmann, M. (2002) Applications of autofluorescence for characterisation of biological systems (biomonitoring). *Biomedizinische Technik* **47 Suppl 1 Pt 2,** 596-597.
12. Yanagita, K., Kamagata, Y., Kawaharasaki, M., Suzuki, T., Nakamura, Y. and Minato, H. (2000) Phylogenetic analysis of methanogens in sheep rumen ecosystem and detection of *Methanomicrobium* by fluorescence in situ hybridization. *Bioscience, Biotechnology, and Biochemistry* **64,** 1737-1742.
13. Yen, G.G. (1994) Identification and control of large structures using neural networks. *Computer and Structures*, 52:859-870.
14. Chinea, G., Padron, P., Hooft, R.W.W., Sander, C. & Vriend, G. (1995). The Use of Position-Specific Rotamers in Model Building by Homology. *Proteins: Structure, Function and Genetics, 23*, 415-421.
15. Hooft, R.W.W., Sander, C. & Vriend, G. (1996) Positioning Hydrogen Atoms by Optimizing Hydrogen-Bond Networks in Protein Structure. *Proteins: Structure, Function and Genetics, 26*, 363-376.

C PUBLICATIONS:

1.) Brian C. Decocq, James T. Blankemeyer, Kristen R. Workman, and Mendel Friedman. Effect of Carvacrol on Autofluorescence, Membrane Potential, and ATP Flux of *Escherichia coli* C600, J. Appl. Microbiol., submitted 2004.
2.) Decocq, B. and G. John. Department of Microbiology & Molecular Genetics, Seminar Series, 2003.

E. STUDENT SUPPORT

1.) Brian Decocq- Master student, Department of Microbiology & Molecular Genetics- Autoflourescence work.
2.) Sanga Venkatraman- Master Student, School of Electrical and Computer Engineering
3.) Sumit Punj-Ph.D. student, Department of Microbiology & Molecular Genetics